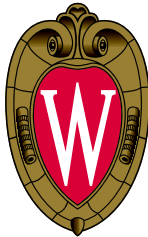# Cyclus Fuel Cycle Simulation Capabilities with the Cyder Disposal System Model

Global 2013

Kathryn D. Huff
katyhuff.github.com

University of Wisconsin-Madison / University of California - Berkeley

October 3, 2013

Motivation
Modeling Capabilities
Conclusion

Future Fuel Cycle Options
Geologic Disposal Concept Options
Fuel Cycle Simulator Capabilities

Outline

Motivation
Modeling Capabilities
Conclusion

Future Fuel Cycle Options
Geologic Disposal Concept Options
Fuel Cycle Simulator Capabilities

Future Fuel Cycle Options

Domestic Fuel Cycle Options

Title	Description	Challenges
Open	Once Through Current US PWR Fleet No Separations No Recycling Higher Burnups	High Temperatures, Volumes
Modified Open	Partial Recycling Next Gen. PWR Fleet Limited Separations Limited Transmutation Advanced Fuel Forms HLW treatment	Both high volumes and variable spent fuel streams
Closed	Full Recycling Full Separations Full Recycling VHTGR, SFRs, other transmutation HLW treatment	Variable spent fuel streams

Table 1 : Domestic Fuel Cycle Options

Motivation
Modeling Capabilities
Conclusion

Future Fuel Cycle Options
Geologic Disposal Concept Options
Fuel Cycle Simulator Capabilities

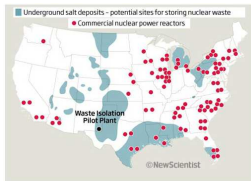## Disposal Geology Options Considered

Figure 1 : U.S. Salt Deposits, ref. [26].
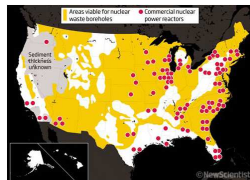

Figure 3 : U.S. Crystalline Basement, ref. [26].

Figure 2 : U.S. Clay Deposits, ref. [11].

Figure 4 : U.S. Granite Beds, ref. [6].

Motivation
Modeling Capabilities
Conclusion

Future Fuel Cycle Options
Geologic Disposal Concept Options
Fuel Cycle Simulator Capabilities
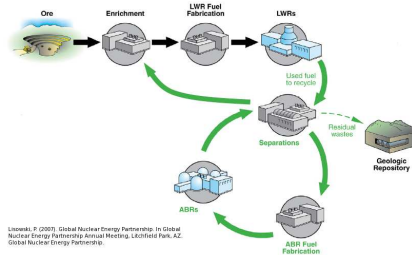
Cyclus Top Level Fuel Cycle Simulator

Figure 5 :   Top level simulators are intended to model the collective behavior of various fuel cycle decisions and strategies [24].

Figure 6 :   cyclus.github.com [17].

Motivation
Modeling Capabilities
Conclusion

Future Fuel Cycle Options
Geologic Disposal Concept Options
Fuel Cycle Simulator Capabilities

Need For an Integrated Repository Model

Repository Capabilities within Systems Analysis Tools

Tool	Institution	Fuel Disposition	Radionuclide Transport	Heat Transport
NUWASTE[2]	NWTRB	yes	no	no
VISION [38]	INL	yes	no	YMR only
DANESS [34]	ANL	no	no	no
COSI [3]	CEA	yes	no	yes
NFCSim [31]	LANL	no	no	no
CAFCA [14]	MIT	no	no	no
ORION [14]	BNL	no	no	no
TSM [33]	OCRWM	yes	no	YMR only

Table 2 :   System tools are lacking in radionuclide transport and heat transport calculations in generic geologic media.

Motivation
Modeling Capabilities
Conclusion

Future Fuel Cycle Options
Geologic Disposal Concept Options
Fuel Cycle Simulator Capabilities

Contributions from This Work

This work has provided a platform capable of bridging the gap between fuel cycle simulation and repository performance analysis.

- Conducted thermal transport sensitivity analyses. [19, 18]
- Conducted contaminant transport sensitivity analyses. [20]
- CYDER acheived integration with a fuel cycle simulator.
- Abstracted physical models of thermal and contaminant transport. [22]
- Demonstrated dominant physics of those models in CYDER, integrated with CYCLUS. [23, 17]
- Published source code, documentation, and testing to facilitate extension by external developers. [21]

Motivation
Modeling Capabilities
Conclusion

Cyder Overview
Radionuclide Transport in Cyder
Thermal Transport in Cyder

Outline

1 Motivation

   Future Fuel Cycle Options
   Geologic Disposal Concept Options
   Fuel Cycle Simulator Capabilities

2 Modeling Capabilities

   Cyder Overview
   Radionuclide Transport in Cyder
   Thermal Transport in Cyder

3 Conclusion

Motivation
Modeling Capabilities
Conclusion

Cyder Overview
Radionuclide Transport in Cyder
Thermal Transport in Cyder

Cyder Paradigm : Waste Stream Acceptance
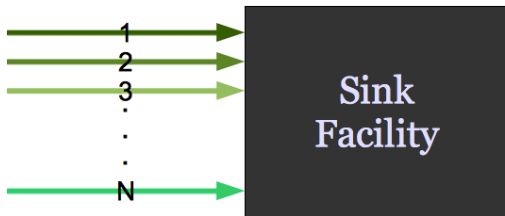
Figure 7 : To participate in a CYCLUS fuel cycle simulation, CYDER must accept **arbitrary** spent fuel and high level waste **material data objects**.

Motivation
Modeling Capabilities
Conclusion

Cyder Overview
Radionuclide Transport in Cyder
Thermal Transport in Cyder

Cyder Paradigm : Waste Stream Conditioning
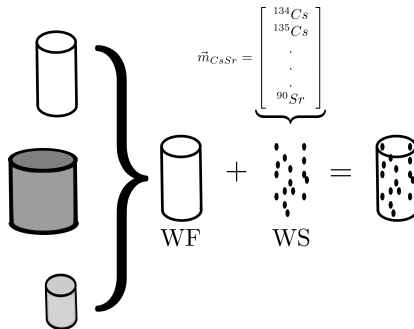
Figure 8 : In Cyder, discrete waste streams are conditioned into the appropriate discrete waste form according to user-specified pairings.
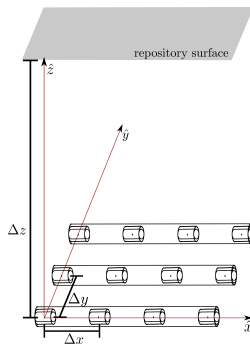
Motivation
Modeling Capabilities
Conclusion

Cyder Overview
Radionuclide Transport in Cyder
Thermal Transport in Cyder

Cyder Paradigm : Waste Form Packaging
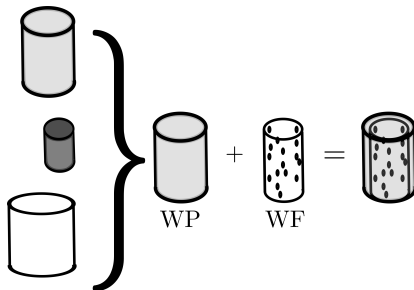
Figure 9 :   In Cyder, one or more waste forms are loaded into the appropriate waste package according to user-specified pairings.

Motivation
Modeling Capabilities
Conclusion

Cyder Overview
Radionuclide Transport in Cyder
Thermal Transport in Cyder

Cyder Paradigm : Waste Package Emplacement

Finally, the waste package is **emplaced** in a buffer component, which contains many other waste packages, spaced evenly in a grid. The grid is defined by the user input and depends on repository depth, Δz, waste package spacing, Δx, and tunnel spacing, Δy as in Figure 10.
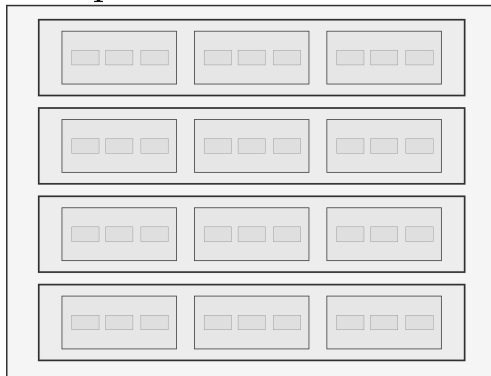
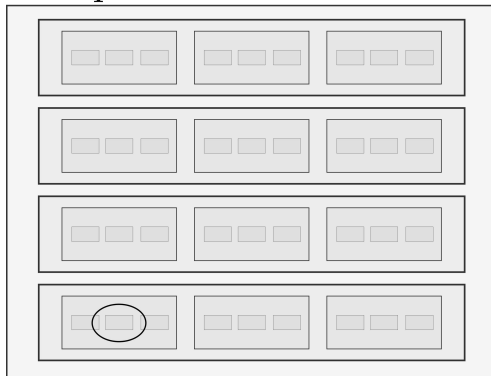Figure 10 : The repository layout has a depth and a uniform package spacing.

Motivation
Modeling Capabilities
Conclusion

Cyder Overview
Radionuclide Transport in Cyder
Thermal Transport in Cyder

Cyder Paradigm : Modularity

Components

Motivation
Modeling Capabilities
Conclusion

Cyder Overview
Radionuclide Transport in Cyder
Thermal Transport in Cyder

Cyder Paradigm : Modularity

Components

Motivation
Modeling Capabilities
Conclusion

Cyder Overview
Radionuclide Transport in Cyder
Thermal Transport in Cyder

Cyder Paradigm : Modularity

Contaminant
Transport
Models

Thermal
Transport
Models

Motivation
Modeling Capabilities
Conclusion

Cyder Overview
Radionuclide Transport in Cyder
Thermal Transport in Cyder

Clay GDSM Sensitivity Analysis

- Barrier Degradation
- Sorption
- Solubility
- Advective Velocity
- Diffusivity
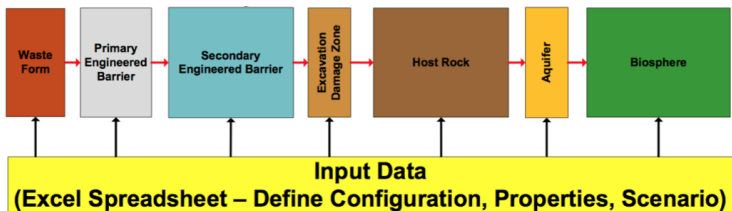
Figure 11 : The Clay Generic Disposal System Model (GDSM) was used for preliminary sensitivity analysis, abstraction iteration, and validation. This figure was reproduced from Figure 3.3-2 in [9].
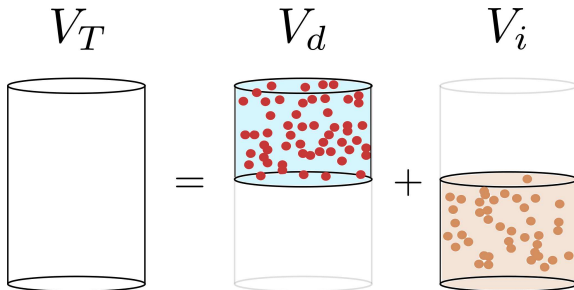
Motivation
Modeling Capabilities
Conclusion

Cyder Overview
Radionuclide Transport in Cyder
Thermal Transport in Cyder

Nested Components

The NuclideModel in a Component can be interchangeably represented by any of the four nuclide transport models.

- Degradation Rate Based Failure Model
- Mixed Cell with Degradation, Sorption, Solubility Limitation
- Lumped Parameter Model
- 1 Dimensional Approximate Advection Dispersion Solution, Brenner [4]

Motivation
Modeling Capabilities
Conclusion

Cyder Overview
Radionuclide Transport in Cyder
Thermal Transport in Cyder
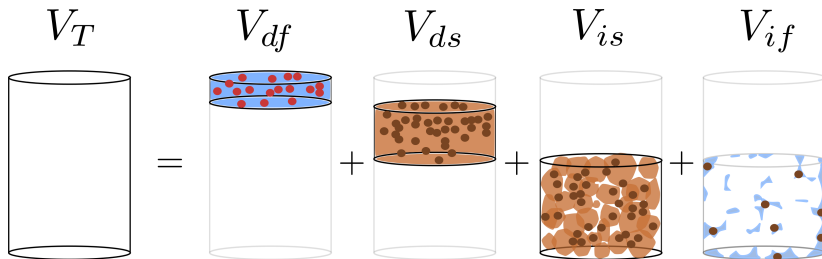
Radionuclide Transport: Degradation Rate Based Release

Figure 12 : The control volume contains an intact volume V_i and a degraded volume, V_d. Contaminants in V_d are available for transport, while contaminants in V_i are contained.

Motivation
Modeling Capabilities
Conclusion

Cyder Overview
Radionuclide Transport in Cyder
Thermal Transport in Cyder

Radionuclide Transport : Mixed Cell with Sorption and Solubility

$$V_T = V_{df} + V_{ds} + V_{is} + V_{if}$$

Figure 13 :   The degraded volume is modeled as a solid degraded volume, V_{ds}, and a fluid degraded volume, V_{df}. The intact volume is modeled as an intact solid volume, V_{is}, and an intact fluid volume V_{if}. Only contaminants in V_{df} are available for transport.

Motivation
Modeling Capabilities
Conclusion

Cyder Overview
Radionuclide Transport in Cyder
Thermal Transport in Cyder

Radionuclide Transport : Mixed Cell Sorption

The mass of contaminant sorbed into the degraded and precipitated solids can be found using a linear isotherm model [32], characterized by the relationship

$$s_i = K_{di} C_i \tag{1}$$

where

$$s_i = \text{the solid concentration of isotope i } [kg/kg]$$
$$K_{di} = \text{the distribution coefficient of isotope i} [m^3/kg]$$
$$C_i = \text{the liquid concentration of isotope i } [kg/m^3].$$

Motivation
Modeling Capabilities
Conclusion

Cyder Overview
Radionuclide Transport in Cyder
Thermal Transport in Cyder

Radionuclide Transport : Mixed Cell Solubility Limitation

In addition to engineered barriers, contaminant transport is constrained by the solubility limit [16],

$$m_{s,i} \leq V_w C_{sol,i}, \tag{2}$$

where

$$m_{s,i} = \text{ solubility limited mass of isotope i in volume } V_w [kg]$$
$$V_w = \text{ volume of the solution } [m^3]$$
$$C_{sol,i} = \text{ solubility limit, the maximum concentration of i } [kg/m^3].$$

Motivation
Modeling Capabilities
Conclusion

Cyder Overview
Radionuclide Transport in Cyder
Thermal Transport in Cyder

Radionuclide Transport: Lumped Parameter Transport Model

C_{in0} $C_{out0} = C_{in1}$ $C_{out1} = C_{in2}$ $C_{out2} = C_{in3}$ C_{out3}
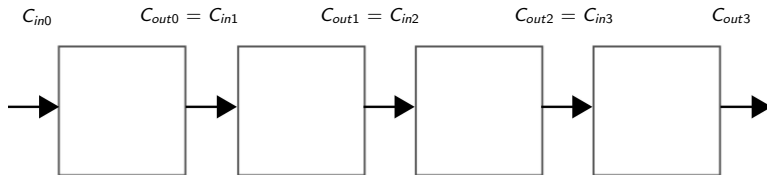
Figure 14 :   The method by which each lumped parameter component is modeled is according to a relationship between the incoming concentration, $C_{in}(t)$, and the outgoing concentration, $C_{out}(t)$.

$$C_{out}(t) = \int_0^\infty C_{in}(t - t')g(t')e^{-\lambda t'}\, dt' \tag{3}$$

where

$$t' = \text{time of entry } [s]$$
$$t - t' = \text{transit time } [s]$$
$$g(t - t') = \text{response function, a.k.a. transit time distribution} [-]$$
$$\lambda = \text{radioactive decay constant} [s^{-1}].$$

Motivation
Modeling Capabilities
Conclusion

Cyder Overview
Radionuclide Transport in Cyder
Thermal Transport in Cyder

Radionuclide Transport: 1D Finite, Cauchy B.C.

$$-D\frac{\partial C}{\partial z}\Big|_{z=0} + vC = \begin{cases} vC_0 & t < t_0 \\ 0 & t > t_0 \end{cases} \qquad \frac{\partial C}{\partial z}\Big|_L = 0$$

$$C(z,0) = C_i$$

$$z = 0 \qquad\qquad\qquad\qquad\qquad\qquad z = L$$

Figure 15 : A one dimensional, finite, unidirectional flow, solution with Cauchy and Neumann boundary conditions [35, 4].

Motivation
Modeling Capabilities
Conclusion

Cyder Overview
Radionuclide Transport in Cyder
Thermal Transport in Cyder

Clay GDSM Degradation Rate Sensitivity
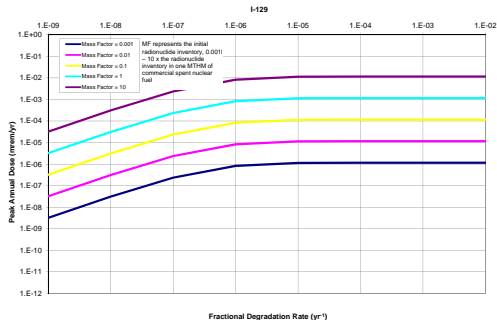
Figure 16 : ^{129}I waste form degradation rate sensitivity.

Motivation
Modeling Capabilities
Conclusion

Cyder Overview
Radionuclide Transport in Cyder
Thermal Transport in Cyder

Cyder Degradation Rate Sensitivity
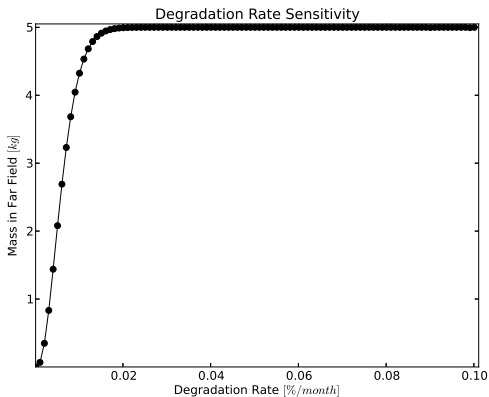
Figure 17 : Sensitivity demonstration of the degradation rate in CYDER for an arbitrary isotope.

Motivation
Modeling Capabilities
Conclusion

Cyder Overview
Radionuclide Transport in Cyder
Thermal Transport in Cyder

Clay GDSM Sorption Sensitivity
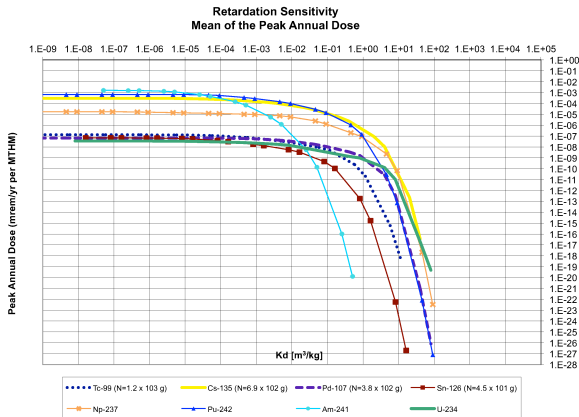
Figure 18 : K_d sensitivity. The peak annual dose due to an inventory, N, of each isotope.

Motivation
Modeling Capabilities
Conclusion

Cyder Overview
Radionuclide Transport in Cyder
Thermal Transport in Cyder

Cyder Sorption Sensitivity
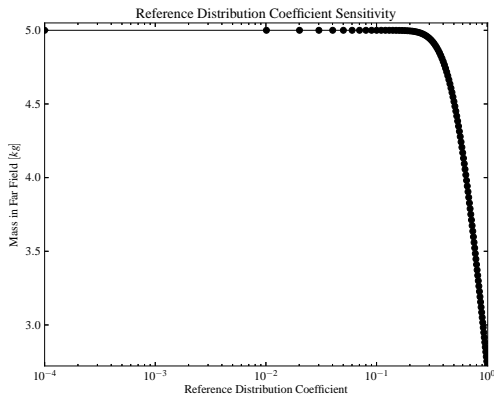
Figure 19 : K_d factor sensitivity in the CYDER tool for an arbitrary isotope assigned a variable K_d coefficient.

Motivation
Modeling Capabilities
Conclusion

Cyder Overview
Radionuclide Transport in Cyder
Thermal Transport in Cyder

Clay GDSM Solubility Sensitivity
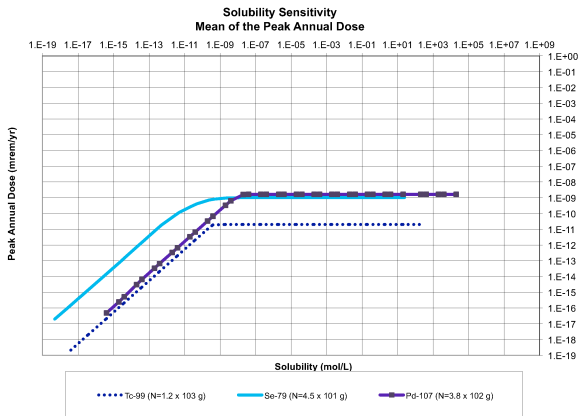
Figure 20 : Solubility limit sensitivity. The peak annual dose due to an inventory, N, of each isotope.

Motivation
Modeling Capabilities
Conclusion

Cyder Overview
Radionuclide Transport in Cyder
Thermal Transport in Cyder

Cyder Solubility Sensitivity
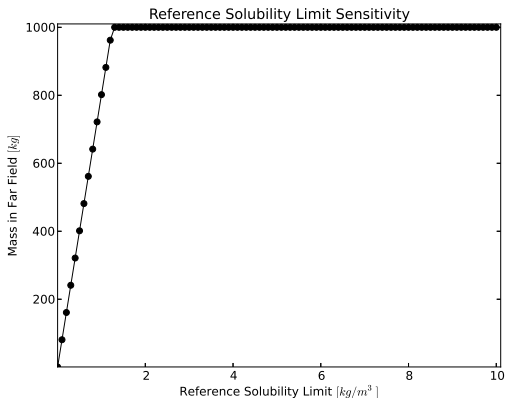
Figure 21 :   Sensitivity demonstration of solubility limitation in CYDER for an arbitrary isotope assigned a variable solubility limit.

Motivation
Modeling Capabilities
Conclusion

Cyder Overview
Radionuclide Transport in Cyder
Thermal Transport in Cyder

Specific Temperature Change Calculations

A reference data set of temperature change curves was calculated. Repeated runs of a detailed model ([15, 13, 12]) over the range of values in Table 4 determined Specific Temperature Change (STC) values over that range.

Thermal Cases

Parameter	Symbol	Units	Value Range
Diffusivity	α_{th}	$[m^2 \cdot s^{-1}]$	$1.0 \times 10^{-7} - 3.0 \times 10^{-6}$
Conductivity	K_{th}	$[W \cdot m^{-1} \cdot K^{-1}]$	$0.1 - 4.5$
Spacing	S	$[m]$	2, 5, 10, 15, 20, 25, 50
Radius	r_{lim}	$[m]$	0.1, 0.25, 0.5, 1, 2, 5
Isotope	i	$[-]$	$^{241,243}Am$, $^{242,243,244,245,246}Cm$, $^{238,240,241,242}Pu$ $^{134,135,137}Cs$ ^{90}Sr

Table 3 :   A thermal reference dataset of STC values as a function of each of these parameters was generated by repeated parameterized runs of the LLNL MathCAD model[12, 13].

Motivation
Modeling Capabilities
Conclusion

Cyder Overview
Radionuclide Transport in Cyder
Thermal Transport in Cyder

Thermal Base Case Demonstration

Specific Temperature Change to LLNL Comparison
(25.9g 242Cm, 0.77g243Cm, 85.6g244Cm, 5.7g245Cm, 7.29g246Cm)
α_{th}=1E-7[m²s⁻¹], K_{th}=2[Wm⁻¹K⁻¹], r_{lim}=50cm, S=2m
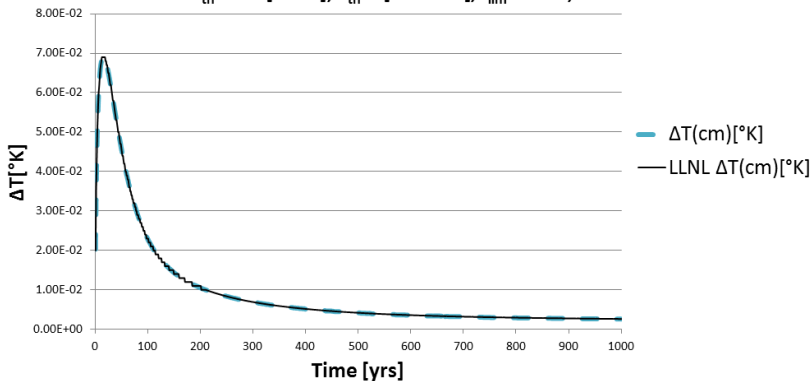
Figure 22 : This comparison of STC calculated thermal response from *Cm* inventory per MTHM in 51GWd burnup UOX PWR fuel compares favorably with results from the semi-analytic model from LLNL.

Motivation
Modeling Capabilities
Conclusion

Cyder Overview
Radionuclide Transport in Cyder
Thermal Transport in Cyder

Thermal Base Case Demonstration
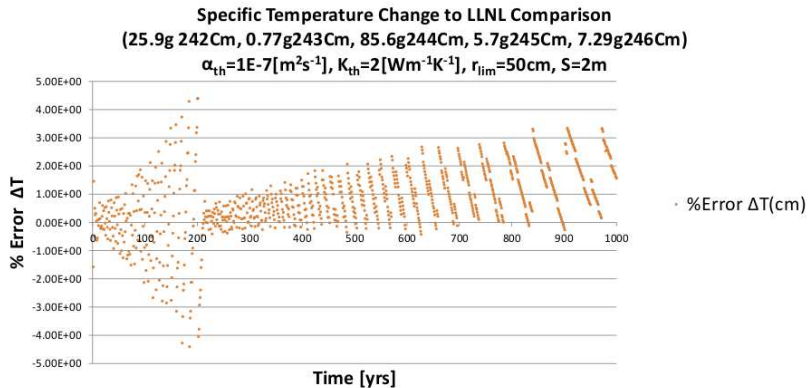
Figure 23 : Percent error between the semi-analytic model from LLNL and the STC calculated thermal response from *Cm* inventory per MTHM in 51GWd burnup UOX PWR fuel demonstrates a maximum percent error of 4.4%.

Motivation
Modeling Capabilities
Conclusion

Cyder Overview
Radionuclide Transport in Cyder
Thermal Transport in Cyder

LLNL Model Thermal Conductivity Sensitivity
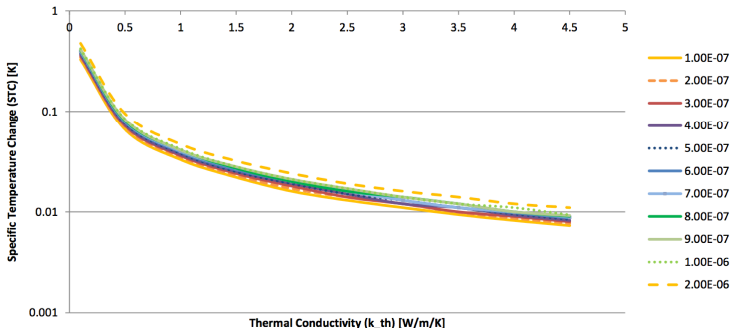
Figure 24 : Increased thermal conductivity decreases the temperature (here represented by STC) at the limiting radius.

Motivation
Modeling Capabilities
Conclusion

Cyder Overview
Radionuclide Transport in Cyder
Thermal Transport in Cyder

Cyder Thermal Conductivity Sensitivity
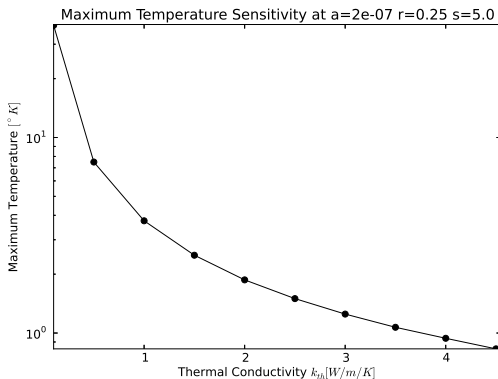
Figure 25 : Cyder results agree with those of the LLNL model. Increased K_{th} decreases temperature change at the limiting radius. The above example thermal profile results from 10kg of ^{242}Cm, $\alpha_{th} = 2 \times 10^{-7}$, $s = 5m$, and $r_{lim} = 0.25m$.

Motivation
Modeling Capabilities
Conclusion

Cyder Overview
Radionuclide Transport in Cyder
Thermal Transport in Cyder

LLNL Model Thermal Diffusivity Sensitivity
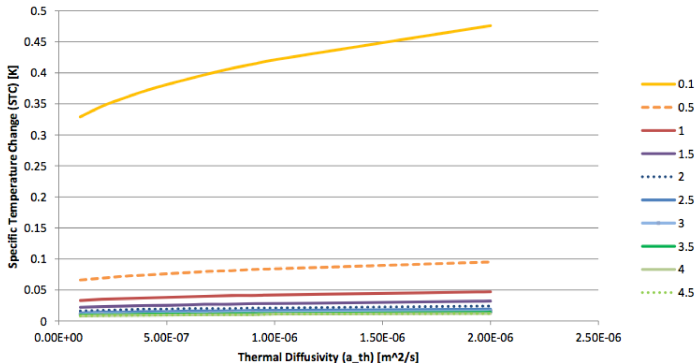
Figure 26 :   Increased thermal diffusivity decreases temperature change (here represented by STC) at the limiting radius (here $r_{calc} = 0.5m$).

Motivation
Modeling Capabilities
Conclusion

Cyder Overview
Radionuclide Transport in Cyder
Thermal Transport in Cyder

Cyder Thermal Diffusivity Sensitivity
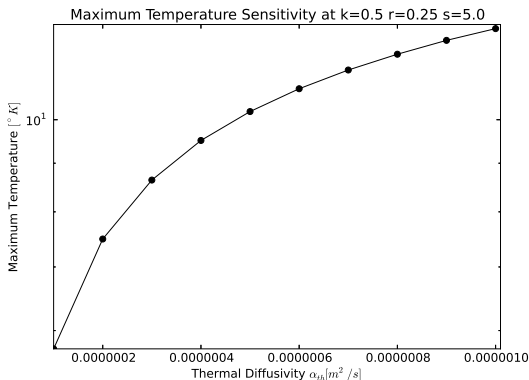
Figure 27 : Cyder trends agree with those of the LLNL model, in which increased thermal diffusivity results in reduced temperature change at the limiting radius. The above example thermal profile results from 10kg of ^{242}Cm.

Outline

Conclusion : Summary of Contributions

This work has provided a software platform capable of bridging the gap between fuel cycle simulation and repository performance analysis.

- Conducted thermal transport sensitivity analyses. [19, 18]
- Conducted contaminant transport sensitivity analyses. [20]
- CYDER acheived integration with a fuel cycle simulator.
- Abstracted physical models of thermal and contaminant transport. [22]
- Demonstrated dominant physics of those models in CYDER, integrated with CYCLUS. [23, 17]
- Published source code, documentation, and testing to facilitate extension by external developers. [21]

Conclusion : Suggested Future Work

Further work could include

- cultivation of a developer community,
- more detailed benchmarking validation against sophisticated tools,
- comparison against experimental data, where available,
- demonstration of dynamic fuel cycle feedback sensitivities,
- additional physics (fracture models, biosphere models),
- and additional supporting data.

Acknowledgements

Figure 28 :   This work relied on CYCLUS, the next generation fuel cycle simulator, and its team. cyclus.github.com

References I

[1] Svensk karnbranslehantering AB.
Long-term Safety for KBS-3 Repositories at Forsmark and Laxemar-a First Evaluation: Main Report of the SR-Can Project.
SKB, November 2006.

[2] Mark Abkowitz.
Nuclear waste assessment system for technical evaluation - NUWASTE, October 2010.

[3] Lionel Boucher.
International comparison for transition scenario codes involving COSI, DESAE, EVOLCODE, FAMILY and VISION, November 2010.
CEA France.

[4] Howard Brenner.
The diffusion model of longitudinal mixing in beds of finite length. numerical values.
Chemical Engineering Science, 17(4):229–243, April 1962.

[5] T.L. Bridges, A.L. Lengyel, D.K. Morton, and D.L. Pincock.
Standardized DOE spent nuclear fuel canister and transportation system for shipment to the national repository.
In *Proceedings of Waste Management 2001*, Tucson, February 2001.

References II

[6]   J. B. Bush.
      Economic and technical feasibility study of compressed air storage.
      Report ERDA, page 7676, 1976.

[7]   H. S. Carslaw and J. C. Jaeger.
      Conduction of heat in solids.
      Oxford: Clarendon Press, 1959, 2nd ed., 1, 1959.

[8]   J. T. Carter, A. J. Luptak, J. Gastelum, C. Stockman, and A. Miller.
      Fuel cycle potential waste inventory for disposition.
      Technical report, FCR&D-USED-2010-000031, Rev. 3, 2011.

[9]   Daniel Clayton, Geoff Freeze, Ernest Hardin, W. Mark Nutt, Jens Birkholzer, H.H. Liu, and
      Shaoping Chu.
      Generic disposal system modeling - fiscal year 2011 progress report.
      Technical Report FCRD-USED-2011-000184, U.S. Department of Energy, Sandia, NM,
      August 2011.

[10] DOE.
      WIPP hazadous waste facility permit community relations plan, 2013.

References III

[11] Serge Gonzales and Kenneth Sutherland Johnson.
Shales and other argillaceous strata in the united states.
Technical report, Earth Resource Associates, Inc., Athens, GA (USA), 1985.

[12] Harris Greenberg, James Blink, Massimiliano Fratoni, Mark Sutton, and Amber Ross.
Application of analytical heat transfer models of multi-layered natural and engineered barriers
in potential high-level nuclear waste repositories.
In *WM2012*, Phoenix, AZ, March 2012.
LLNL-CONF-511672.

[13] Harris Greenberg, Montu Sharma, and Mark Sutton.
Investigations on repository near-field thermal modeling.
Technical report, Lawrence Livermore National Laboratory, 2012.

[14] Laurent Guerin.
A Benchmark Study of Computer Codes for System Analysis of the Nuclear Fuel Cycle,
volume MIT-NFC-TR-105.
Massachusetts Institute of Technology. Center for Advanced Nuclear Energy Systems. Nuclear
Fuel Cycle Program, 2009.

References IV

[15] Ernest Hardin, James Blink, Harris Greenberg, Mark Sutton, Massimo Fratoni, Joe Carter, Mark Dupont, and Rob Howard.
Generic repository design concepts and thermal analysis - 8.8.2011 draft.
Technical Report FCRD-USED-2011-000143, Department of Energy Office of Used Fuel Disposition, Sandia, August 2011.

[16] A. Hedin.
Integrated analytic radionuclide transport model for a spent nuclear fuel repository in saturated fractured rock.
Nuclear Technology, 138(2), 2002.

[17] Kathryn Huff.
Cyclus fuel cycle simulation capabilities with the cyder disposal system model (in press).
In *Proceedings of GLOBAL 2013*, Salt Lake City, UT, United States, October 2013.

[18] Kathryn Huff and Theodore H. Bauer.
Benchmarking a new closed-form thermal analysis technique against a traditional lumped parameter, finite-difference method.
Technical Report FCRD-UFD-000142, Argonne National Laboratory, Argonne, IL, United States, July 2012.

References V

[19] Kathryn Huff and Theodore H. Bauer.
Numerical calibration of an analytical generic nuclear repository heat transfer model.
In *Transactions of the American Nuclear Society*, volume 106 of *Modeling and Simulation in the Fuel Cycle*, pages 260—263, Chicago, IL, United States, June 2012. American Nuclear Society, La Grange Park, IL 60526, United States.

[20] Kathryn Huff and Mark Nutt.
Key processes and parameters in a generic clay disposal system model.
In *Transactions of the American Nuclear Society*, volume 107 of *Environmental Sciences – General*, pages 208—211, San Diego, CA, November 2012. the American Nuclear Society.

[21] Kathryn D. Huff.
Cyder : A generic geology repository performance library, 2013.

[22] Kathryn D. Huff.
Hydrologic nuclide transport models in cyder, a geologic disposal software library.
In *WM2013*, Phoenix, AZ, February 2013. Waste Management Symposium.

References VI

[23] Kathryn D. Huff and Alexander T. Bara.
Dynamic determination of thermal repository capacity for fuel cycle analysis.
In *Transactions of the American Nuclear Society*, volume 108, pages 123–126, Atlanta, GA, United States, June 2013.

[24] P. Lisowski.
Global nuclear energy partnership.
In *Global Nuclear Energy Partnership Annual Meeting*, 2007.

[25] Piotr Maloszewski and Andrzej Zuber.
Lumped parameter models for the interpretation of environmental tracer data.
Manual on mathematical models in isotope hydrology. IAEA-TECDOC-910, page 959, 1996.

[26] NewScientist.
Where should the US store its nuclear waste?
NewScientist, April 2011.

[27] Christophe Poinssot and Stphane Gin.
Long-term behavior science: The cornerstone approach for reliably assessing the long-term performance of nuclear waste.
Journal of Nuclear Materials, 420(13):182–192, January 2012.

References VII

[28] ptc.
MathCAD engineering calculations software, 2010.

[29] T. E Radel.
Repository modeling for fuel cycle scenario analysis.
University of Wisconsin – Madison, 2007.

[30] Tracy E. Radel, Paul P.H. Wilson, R. M. Grady, and Theodore H. Bauer.
Effect of separation efficiency on repository loading values in fuel cycle scenario analysis codes.
American Nuclear Society, LaGrange Park, IL, 2007.

[31] E. Schneider, M. Knebel, and W. Schwenk-Ferrero.
NFCSim scenario studies of german and european reactor fleets.
Technical report, LA-UR-04-4911, Los Alamos National Laboratory, 2004.

[32] F. W. Schwartz and H. Zhang.
Fundamentals of ground water.
Environmental Geology, 45:10371038, 2004.

References VIII

[33] Stephen L. Turner.
Discrete modeling: OCRWM total system model DRAFT.
Fuel Cycle Technologies FCR&D-XXXX-2009-XXXXXX, Argonne National Laboratory,
Argonne, IL, United States, May 2010.

[34] L. Van Den Durpel, D. C. Wade, and Abdellatif Yacout.
DANESS: a system dynamics code for the holistic assessment of nuclear energy system
strategies.
Proceedings of the 2006 System Dynamics Conference, 2006.

[35] Martinus Th. Van Genuchten and W. J. Alves.
Analytical solutions of the one-dimensional convective-dispersive solute transport equation.
Technical Bulletin, 9(1661), 1982.

[36] W. von Lensa, R. Nabbi, and M. Rossbach.
RED-IMPACT Impact of Partitioning, Transmutation and Waste Reduction Technologies on
the Final Nuclear Waste Disposal.
Forschungszentrum Julich, 2008.

References IX

[37] Herbert Fan Wang and Mary P. Anderson.
Introduction to groundwater modeling.
Academic Press, 1982.

[38] A. M. Yacout, J. J. Jacobson, G. E. Matthern, S. J. Piet, D. E. Shropshire, and C. Laws.
VISION – verifiable fuel cycle simulation of nuclear fuel cycle dynamics.
In *Waste Management Symposium*, 2006.
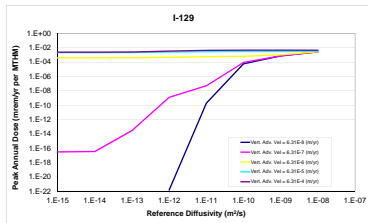
GDSM Model Advective Diffusive Sensitivity
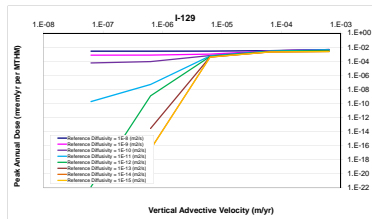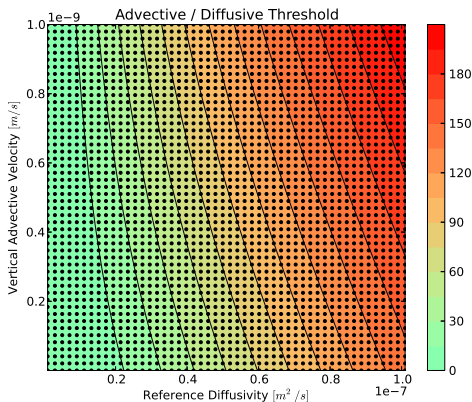

Figure 29 : ^{129}I reference diffusivity sensitivity.

Figure 30 : ^{129}I vertical advective velocity sensitivity.

Cyder Advective Diffusive Sensitivity

Figure 31 :   Dual advective velocity and reference diffusivity sensitivity for a non-sorbing, infinitely soluble nuclide. This demonstration utilized the Degradation Rate model and the coupled advective dispersive mass transfer mode.

Outline

4 **Thermal Methodology**

5 Nuclide Transport Methodology

6 LLNL Model Background
   Analytical Model Background

7 Geologic Media and Concepts

8 Mixed Cell Model

Thermal Modeling in Cyder

Two types of thermal modeling occur in Cyder.

- The first is **capacity estimation** for waste stream acceptance.
- The next is **heat evolution** which determines heat evolution in the modules over repository lifetime.

Thermal Modeling in Cyder

Each can be acheived with one thermal model,

- This model employs a Specific Temperature Change algorithm [30, 29] and

- relies on a supporting **response database** combining detailed spent nuclear fuel composition data [8] with a detailed thermal repository performance analysis tool from Lawrence Livermore National Lab (LLNL) and the Used Fuel Disposition (UFD) campaign [12].

- This method is capable of rapid estimation of temperature increase near emplacement tunnels as a function of
  - waste composition,
  - limiting radius, r_{lim},
  - waste package spacing, S,
  - near field thermal conductivity, K_{th},
  - and near field thermal diffusivity, α_{th}.

Specific Temperature Change Method

Introduced by Radel, Wilson et al., the Specific Temperature Change (STC) method uses a linear approximation to arrive at the thermal loading density limit [29, 30].

First, ΔT is determined for a limiting loading density of the particular material composition then it is normalized to a single kilogram of that material, Δt, the so called STC.

$$\Delta T(r_{lim}) = m \cdot \Delta t(r_{lim}) \qquad (4)$$

where

$$\begin{aligned}
\Delta T &= \text{Temperature change due to m } [K] \\
m &= \text{Mass of heat generating material } [kg] \\
\Delta t &= \text{Temperature change due to 1 kg } [K/kg] \\
r_{lim} &= \text{Limiting radius } [m].
\end{aligned}$$

Specific Temperature Change Superposition

For an arbitrary waste stream composition, scaled curves, Δt_i, calculated in this manner for individual isotopes can be superimposed for each isotope to arrive at an approximate total temperature change.

$$\Delta T(r_{lim}) \sim \sum_i m_i \Delta t_i(r_{lim}) \tag{5}$$

where

$$
\begin{aligned}
i &= \text{An isotope in the material } [-] \\
m_i &= \text{mass of isotope i } [kg] \\
\Delta t_i &= \text{Specific temperature change due to } i \ [K].
\end{aligned}
$$

LLNL UFD MathCAD Model

The analytic model used to populate the reference dataset was created at LLNL for the UFD campaign [15, 13, 12]. It employs an analytic model from Carslaw and Jaeger and is **implemented in MathCAD** [7, 28]. The integral solver in the MathCAD toolset is the primary calculation engine for the analytic MathCAD thermal model, which relies on superposition of point, finite-line, and line source integral solutions.

Specific Temperature Change Calculations

A reference data set of temperature change curves was calculated. Repeated runs of a detailed model over the range of values in Table 4 determined Specific Temperature Change (STC) values over that range.

Thermal Cases

Parameter	Symbol	Units	Value Range
Diffusivity	α_{th}	$[m^2 \cdot s^{-1}]$	$1.0 \times 10^{-7} - 3.0 \times 10^{-6}$
Conductivity	K_{th}	$[W \cdot m^{-1} \cdot K^{-1}]$	$0.1 - 4.5$
Spacing	S	$[m]$	2, 5, 10, 15, 20, 25, 50
Radius	r_{lim}	$[m]$	0.1, 0.25, 0.5, 1, 2, 5
Isotope	i	$[-]$	$^{241,243}Am$, $^{242,243,244,245,246}Cm$, $^{238,240,241,242}Pu$ $^{134,135,137}Cs$ ^{90}Sr

Table 4 : A thermal reference dataset of STC values as a function of each of these parameters was generated by repeated parameterized runs of the LLNL MathCAD model[12, 13].

Scaling Demonstration

Specific Temperature Change Scaling Calculation (25.9g 242Cm)
α_{th}=1E-7[m^{2}s^{-1}], K_{th}=2[Wm^{-1}K^{-1}], r_{lim}=50cm, S=2m
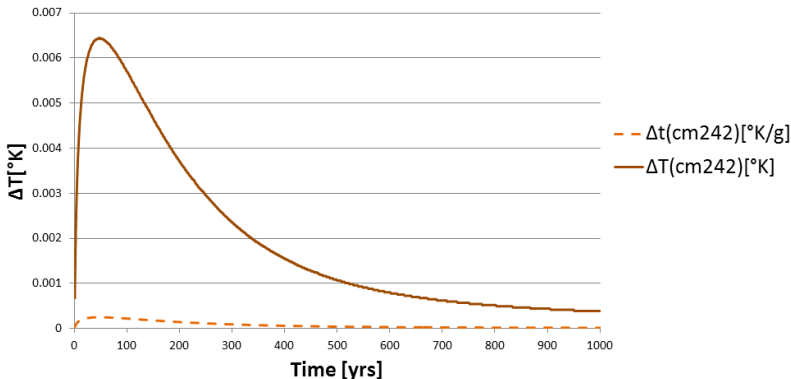
Figure 32 : As a demonstration of the calculation procedure, the temperature change curve for one initial gram of ^{242}Cm and is scaled to represent 25.9g, approximately the ^{242}Cm inventory per MTHM in 51GWd burnup UOX PWR fuel.

Superposition Concept

The supporting database was limited to some primary heat contributing isotopes present in traditional spent nuclear fuel, H, such that the superposition in equation (5) becomes

$$\Delta T(r_{lim}, S, K_{th}, \alpha_{th}) \sim \sum_{i \in H} m_i \Delta t_i(r_{lim}, S, K_{th}, \alpha_{th}) \tag{6}$$

where

$$
\begin{aligned}
H &= \text{ set of high heat isotopes } [-] \\
S &= \text{ uniform waste package spacing } [m] \\
K_{th} &= \text{ thermal conductivity } [W \cdot m^{-1} \cdot K^{-1}] \\
\alpha_{th} &= \text{ thermal diffusivity } [m^2 \cdot s^{-1}]
\end{aligned}
$$

$$\tag{7}$$

Superposition Demonstration

Specific Temperature Change Superposition Calculation
(25.9g 242Cm, 0.77g243Cm, 85.6g244Cm, 5.7g245Cm, 7.29g246Cm)
α_{th}=1E-7[m^2s^{-1}], K_{th}=2[$Wm^{-1}K^{-1}$], r_{lim}=50cm, S=2m

- - - ΔT(cm242)[°K]
······ ΔT(cm243)[°K]
······ ΔT(cm244)[°K]
-·-· ΔT(cm245)[°K]
— ΔT(cm246)[°K]
—— ΔT(cm)[°K]
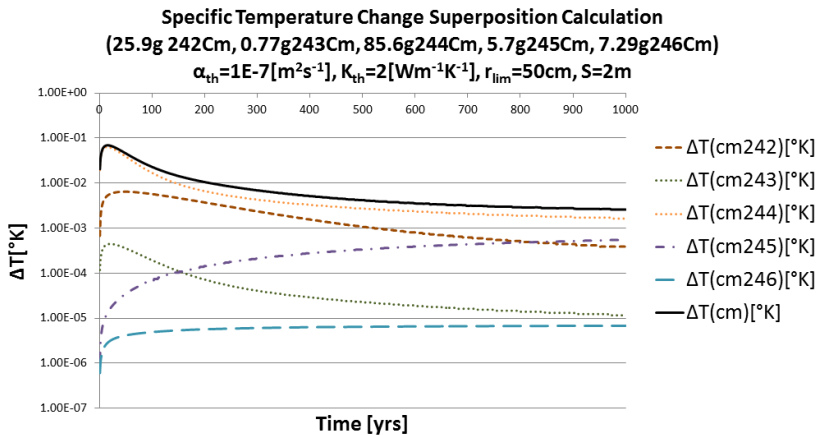
Figure 33 : As a demonstration of the calculation procedure, scaled temperature change curves for five curium isotopes are superimposed to achieve a total temperature change (note log scale).

Outline

4 Thermal Methodology

5 Nuclide Transport Methodology

6 LLNL Model Background
   Analytical Model Background

7 Geologic Media and Concepts

8 Mixed Cell Model

Timestepping Algorithm
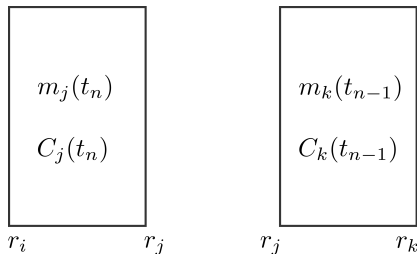
Figure 34 :   Two components share an interface at r_j and contain mass and concentration profiles at the beginning of timestep t_n.
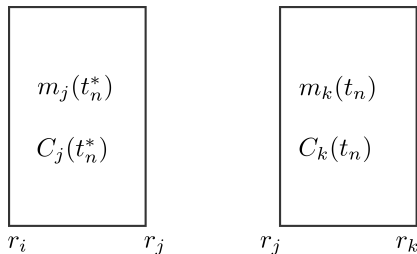
Timestepping Algorithm
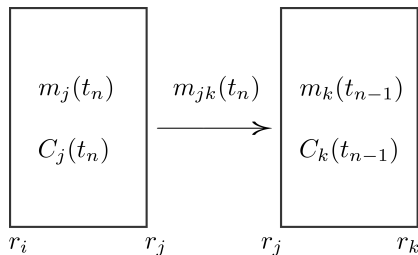
Figure 35 : The mass balance model in component k calculates the appropriate mass transfer based on boundary information from component j.

Timestepping Algorithm

Figure 36 : Based on the mass transfer, both components update their mass and concentration profiles based on their mass balance model.

Advection Dispersion Equation

In a saturated, reducing environment, contaminants are transported by **dispersion** and **advection** [32, 37, 35]:

$$
\begin{aligned}
J &= J_{dis} + J_{adv} \\
&= -\theta(D_{mdis} + \tau D_m)\nabla C + \theta v C \\
&= -\theta D \nabla C + \theta v C
\end{aligned}
$$

$$(8)$$

where

$$
\begin{aligned}
J_{dis} &= \text{Total Dispersive Mass Flux } [kg/m^2/s] \\
J_{adv} &= \text{Advective Mass Flux } [kg/m^2/s] \\
\tau &= \text{Toruosity } [-] \\
\theta &= \text{Porosity } [-] \\
D_m &= \text{Molecular diffusion coefficient } [m^2/s] \\
D_{mdis} &= \text{Coefficient of mechanical dispersivity} [m^2/s] \\
D &= \text{Effective Dispersion Coefficient } [m^2/s] \\
C &= \text{Concentration } [kg/m^3] \\
v &= \text{Fluid Velocity in the medium } [m/s].
\end{aligned}
$$

Radionuclide Transport: Lumped Parameter Transport Model

C_{in0} $C_{out0} = C_{in1}$ $C_{out1} = C_{in2}$ $C_{out2} = C_{in3}$ C_{out3}
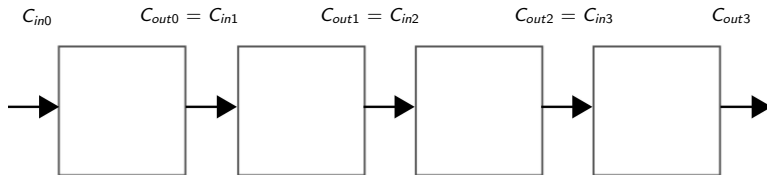
Figure 37 : The method by which each lumped parameter component is modeled is according to a relationship between the incoming concentration, $C_{in}(t)$, and the outgoing concentration, $C_{out}(t)$.

$$C_{out}(t) = \int_0^\infty C_{in}(t - t')g(t')e^{-\lambda t'}\,dt' \tag{9}$$

where

$$t' = \text{time of entry [s]}$$
$$t - t' = \text{transit time [s]}$$
$$g(t - t') = \text{response function, a.k.a. transit time distribution}[-]$$
$$\lambda = \text{radioactive decay constant}[s^{-1}].$$

Radionuclide Transport: Lumped Parameter Transport Model

Some response functions used commonly in chemical engineering applications include the Piston Flow Model (PFM), Exponential Model (EM), and the dispersion model (DM). The solutions to these for constant concentration at the source boundary are given in [25],

$$
C(t) = \begin{cases} PFM & C_0 e^{-\lambda t_t} \\ EM & \frac{C_0}{1 + \lambda t_t} \\ DM & C_0 e^{\frac{Pe}{2}\left(1 - \sqrt{1 + \frac{4\lambda t_t}{Pe}}\right)}. \end{cases} \tag{10}
$$

Lumped Parameter Model Base Case
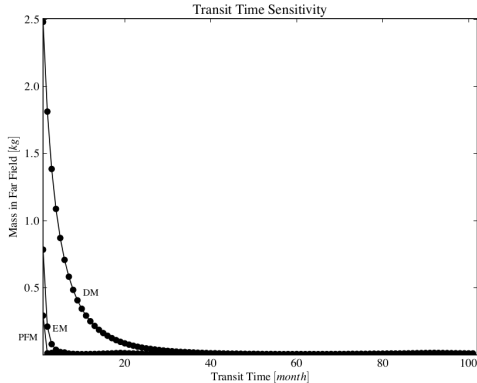
Figure 38 : The transit time parameterization of the lumped parameter model has a strong effect on the material reaching the far field after 30 months. The choice of model also strongly affects the results.

Radionuclide Transport: 1D Finite, Cauchy B.C.

For the boundary conditions,

$$-D\frac{\partial C}{\partial z}\Big|_{z=0} + v_z c = \begin{cases} v_z C_0 & (0 < t < t_0) \\ 0 & (t > t_0) \end{cases} \tag{11}$$

and

$$\frac{\partial C}{\partial z}\Big|_{z=L} = 0 \tag{12}$$

and the initial condition,

$$C(z,0) = C_i, \tag{13}$$

the solution is given as

$$C(z,t) = \begin{cases} C_i + (C_0 - C_i)\,A(z,t) & 0 < t \le t_0 \\ C_i + (C_0 - C_i)\,A(z,t) - C_0 A(z, t-t_0) & t \ge t_0. \end{cases} \tag{14}$$

Radionuclide Transport: 1D Finite, Cauchy B.C.

For the vertical flow coordinate system, A is defined as

$$
\begin{aligned}
A(z, t) =\ & \left(\frac{1}{2}\right) \operatorname{erfc}\left[\frac{Rz - vt}{2\sqrt{DRt}}\right] \\
& + \left(\frac{v^2 t}{\pi RD}\right)^{1/2} \exp\left[-\frac{(Rz - vt)^2}{4DRt}\right] \\
& - \frac{1}{2}\left(1 + \frac{vz}{D} + \frac{v^2 t}{DR}\right) \exp\left[\frac{vz}{D}\right] \operatorname{erfc}\left[\frac{Rz + vt}{2\sqrt{DRt}}\right] \\
& + \left(\frac{4v^2 t}{\pi RD}\right)^{1/2}\left[1 + \frac{v}{4D}\left(2L - z + \frac{vt}{R}\right)\right] \exp\left[\frac{vL}{D} - \frac{R}{4Dt}\left(2L - z + \frac{vt}{R}\right)^2\right] \\
& - \frac{v}{D}\left[2L - z + \frac{3vt}{2R} + \frac{v}{4D}\left(2L - z + \frac{vt}{R}\right)^2\right] \exp\left[\frac{vL}{D}\right] \operatorname{erfc}\left[\frac{R(2L - z) + vt}{2\sqrt{DRt}}\right]
\end{aligned}
$$

where

$L =$ Extent of the solution domain $[m]$

$R =$ Retardation factor $[-]$.

Thermal Methodology
Nuclide Transport Methodology
LLNL Model Background
Geologic Media and Concepts
Mixed Cell Model

Analytical Model Background

Outline

4 Thermal Methodology

5 Nuclide Transport Methodology

6 LLNL Model Background
  Analytical Model Background

7 Geologic Media and Concepts

8 Mixed Cell Model

Thermal Methodology
Nuclide Transport Methodology
LLNL Model Background
Geologic Media and Concepts
Mixed Cell Model

Analytical Model Background

Analytical Model : Background

The analytical model
- was created at LLNL (H. Greenberg, J. Blink, et. al) [15, 13, 12]
- employs an analytic model from Carslaw and Jaeger [7]
- is implemented in MathCAD [28]
- seeks to inform heat limited waste capacity calculations for
  - arbitrary geology
  - arbitrary waste package loading densities
  - arbitrary homogeneous decay heat source

Thermal Methodology
Nuclide Transport Methodology
LLNL Model Background
Geologic Media and Concepts
Mixed Cell Model

Analytical Model Background

Analytical Model : Geometry
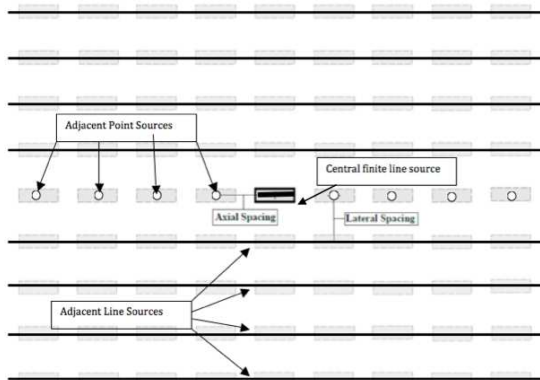
Figure 39 : Vertical, horizontal, alcove, and borehole emplacement layouts can be represented by a line of point sources and adjacent line sources [13].

Thermal Methodology
Nuclide Transport Methodology
LLNL Model Background
Geologic Media and Concepts
Mixed Cell Model

Analytical Model Background

Analytical Model : Calculation Method

LLNL's model is a MathCAD solution of the transient homogeneous conduction equation,

$$\nabla^2 T = \frac{1}{\alpha} \frac{\partial T}{\partial t}, \tag{15}$$

in which superimposed point and line source solutions approximate the repository layout.

Thermal Methodology
Nuclide Transport Methodology
LLNL Model Background
Geologic Media and Concepts
Mixed Cell Model

Analytical Model Background

Analytical Model : Calculation Method

The model consists of two conceptual regions, an external region representing
the host rock and an internal region representing the waste form, package, and
buffer Engineered Barrier System within the disposal tunnel wall.

- Since the thermal mass of the EBS is small in comparison to the thermal
  mass of the host rock, the internal region may be treated as quasi-steady
  state.

- The transient state of the temperature at the calculation radius is found
  with a convolution of the transient external solution with the steady state
  internal solution.

- The internal and external regions are **approximated** to be a single
  homogeneous medium.

- The process is then iterated with a one year resolution in order to arrive at
  a temperature evolution over the lifetime of the repository.

Thermal Methodology
Nuclide Transport Methodology
LLNL Model Background
Geologic Media and Concepts
Mixed Cell Model

Analytical Model Background

Analytical Model : Calculation Method
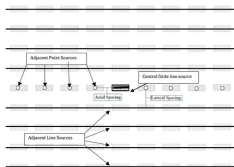
Figure 40 : The central package is represented by a finite line source [13].

The geometric layout of the analytic LLNL model in Figure 42 shows that the central package is represented by the finite line solution

$$T_{line}(t, x, y, z) =$$

$$\frac{1}{8\pi K_{th}} \int_0^t \frac{q_L(t')}{t - t'} e^{\frac{-\left(x^2 + z^2\right)}{4\alpha(t - t')}}$$

$$\cdot \left[\text{erf}\left[\frac{1}{2} \frac{\left(y + \frac{L}{2}\right)}{\sqrt{\alpha(t - t')}} \right] - \text{erf}\left[\frac{1}{2} \frac{\left(y - \frac{L}{2}\right)}{\sqrt{\alpha(t - t')}} \right] \right] \, \mathrm{d}t'.$$

$$(16)$$

Thermal Methodology
Nuclide Transport Methodology
LLNL Model Background
Geologic Media and Concepts
Mixed Cell Model

Analytical Model Background

Analytical Model : Calculation Method
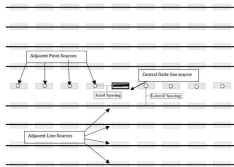
Figure 41 : Adjacent packages are represented as point sources [13].

Adjacent packages within the central tunnel are represented by the point source solution,

$$T_{point}(t, r) = \frac{1}{8K_{th}\sqrt{\alpha}\pi^{\frac{3}{2}}}$$

$$\int_0^t \frac{q(t')}{(t - t')^{\frac{3}{2}}} e^{\frac{-r^2}{4\alpha(t-t')}} \, \mathrm{d}t'. \qquad (17)$$

Thermal Methodology
Nuclide Transport Methodology
LLNL Model Background
Geologic Media and Concepts
Mixed Cell Model

Analytical Model Background

Analytical Model : Calculation Method
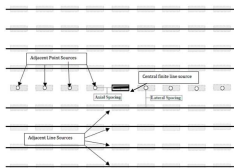
Figure 42 : The non-central disposal tunnels are represented as infinite line sources [13].

Adjacent disposal tunnels are represented by the infinite line source solution,

$$T_{\infty\,line}(t,x,z) = \frac{1}{4\pi K_{th}} \int_0^t \frac{q_L(t')}{t-t'} e^{\frac{-\left(x^2+z^2\right)}{4\alpha(t-t')}} \qquad (18)$$

in infinite homogeneous media, where

$$\alpha = \quad \text{thermal diffusivity } [m^2 \cdot s^{-1}]$$

$$q(t) = \quad \text{point heat source}[W]$$

and

$$q_L(t) = \quad \text{linear heat source}[W \cdot m^{-1}]$$

Superimposed point and line source solutions allow for a notion of the repository layout to be modeled in the host rock.

Outline

4. Thermal Methodology

5. Nuclide Transport Methodology

6. LLNL Model Background
   Analytical Model Background

7. **Geologic Media and Concepts**

8. Mixed Cell Model

Repository Components
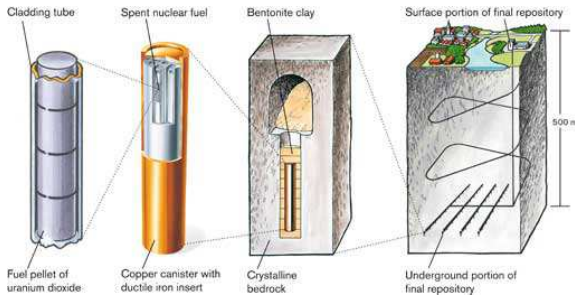
Figure 43 : Geologic disposal systems typically employ engineered barrier systems as well as natural barrier systems. This is a Swedish concept in granite [1].

Clay Disposal Environments
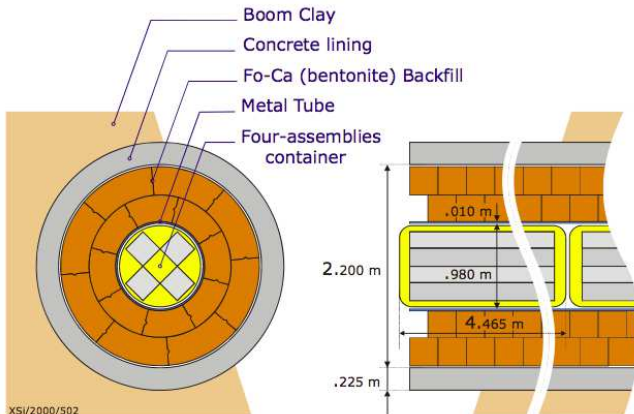
Figure 44 : Belgian reference concept in Boom Clay [36].

Granite Disposal Environments
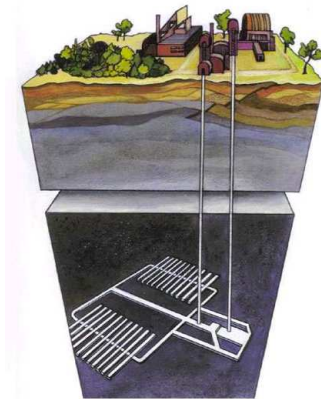
Figure 45 :   Czech reference concept in Granite [36].

Salt Disposal Environments

Figure 46 : DOE-NE Used Fuel Disposition Campaign concept in Salt [15].

Salt Disposal Environments
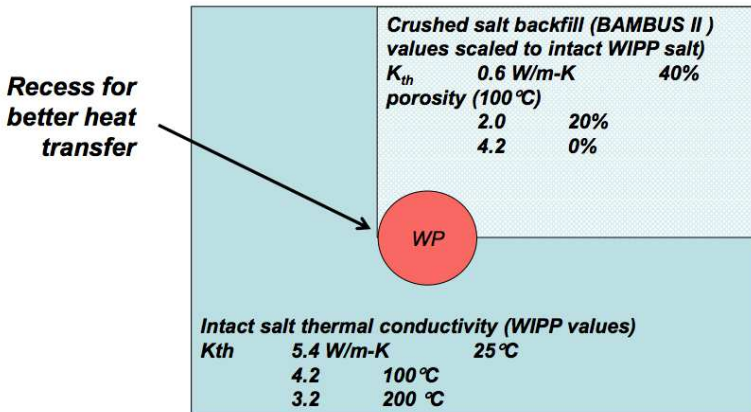
Figure 47 : DOE-NE Used Fuel Disposition Campaign concept in Salt [15].

Deep Borehole Disposal Environment
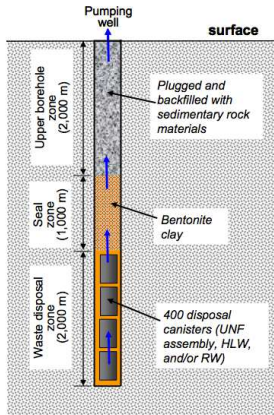
Figure 48 : DOE-NE Used Fuel Disposition Campaign Deep Borehole concept [15].

Engineered Barriers : Waste Forms

The first line of defense is the waste form.
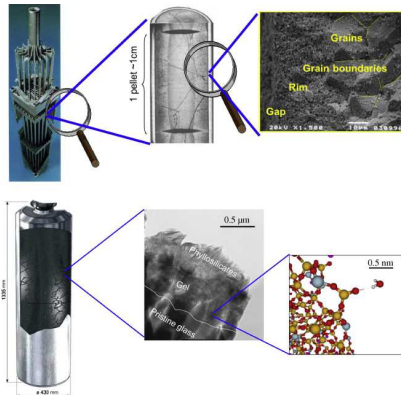
Figure 49 : A comparison of uranium oxide and borosilicate glass waste forms [27].

Engineered Barriers : Waste Packages
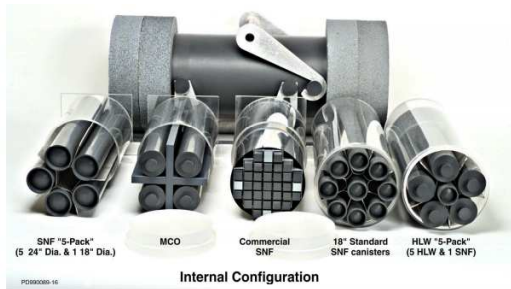
Figure 50 : Conceptual mockup of waste packages around waste forms [5].

Engineered Barriers : Disposal Cask
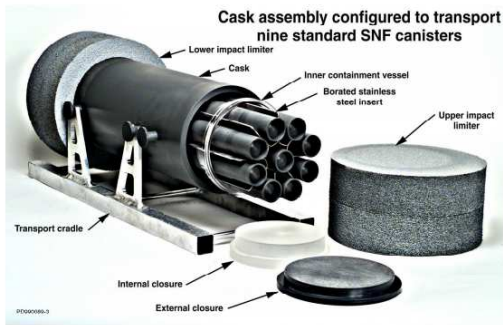
Figure 3. Conceptual design model.

Figure 51 :   Conceptual mockup of a transport and disposal cask [5].

Engineered Barriers : Buffer

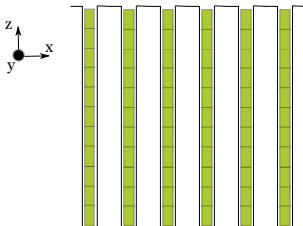Figure 52 : Belgian reference concept in Boom Clay [36].

Natural Barrier : Geology
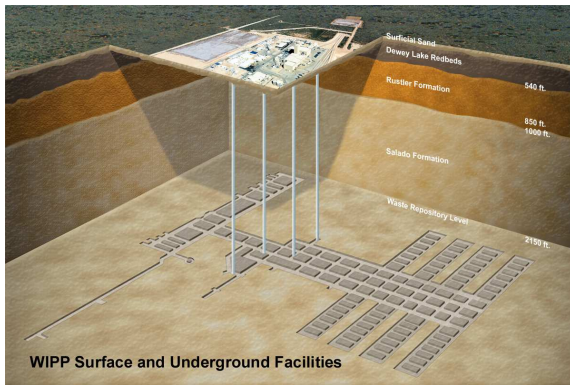
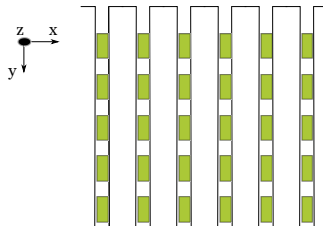Figure 53 :   The Waste Isolation Pilot Plant has many geologic layers above the salt
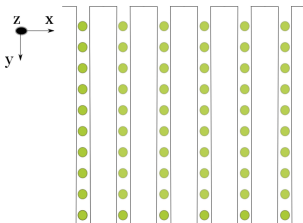bed [10].

Repository Layouts

Deep Boreholes

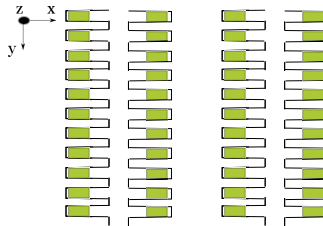Horizontal In-Tunnel

Vertical In-Tunnel

Alcoves

Outline

4 Thermal Methodology

5 Nuclide Transport Methodology

6 LLNL Model Background
   Analytical Model Background

7 Geologic Media and Concepts

8 Mixed Cell Model

Radionuclide Transport : Mixed Cell Sorption

The mass of contaminant sorbed into the degraded and precipitated solids can be found using a linear isotherm model [32], characterized by the relationship

$$s_i = K_{di} c_i \tag{19}$$

where

$$s_i = \text{the solid concentration of isotope i } [kg/kg]$$

$$K_{di} = \text{the distribution coefficient of isotope i} [m^3/kg]$$

$$c_i = \text{the liquid concentration of isotope i } [kg/m^3].$$

From the sorbed contaminant mass, we find the non-sorbed contaminant mass in the free fluid,

$$m_{ffl} = m_{ffT} - \frac{1}{2} \left(m_{ffT} - m_{psm} - \frac{V_{ff}}{K_d} \right)$$
$$\mp \frac{1}{2} \sqrt{ m_{ffT}^2 + 2 m_{ffT} \left(m_{psm} - \frac{V_{ff}}{K_d} \right) + \left(m_{psm} + \frac{V_{ff}}{K_d} \right)^2 }. \tag{20}$$

where

$$m_{ffT} = \text{total degraded contaminant mass } [kg]$$

$$m_{psm} = \text{noncontaminant mass in degraded and precipitated solids } [kg]$$

$$m_{psc} = \text{contaminant mass in degraded and precipitated solids } [kg]$$

$$\rho_b = \text{bulk (dry) density of the medium } [kg/m^3].$$

$$\tag{21}$$